Petasin Activates AMP-Activated Protein Kinase and Modulates Glucose Metabolism

ARTICLE *in* JOURNAL OF NATURAL PRODUCTS · MAY 2014

Impact Factor: 3.8 · DOI: 10.1021/np400867m · Source: PubMed

8 AUTHORS, INCLUDING:

Tetsuya Takimoto
Ajinomoto Group
9 PUBLICATIONS **95** CITATIONS
SEE PROFILE

Katsuya Suzuki
Ajinomoto Group
25 PUBLICATIONS **394** CITATIONS
SEE PROFILE

Tetsuya Miwa
AJINOMOTO CO., INC.
20 PUBLICATIONS **383** CITATIONS
SEE PROFILE

Yasushi Noguchi
AJINOMOTO CO., INC.
33 PUBLICATIONS **475** CITATIONS
SEE PROFILE

JOURNAL OF NATURAL PRODUCTS

Article

pubs.acs.org/jnp

Petasin Activates AMP-Activated Protein Kinase and Modulates Glucose Metabolism

Yusuke Adachi, Yayoi Kanbayashi, Ikue Harata, Risa Ubagai, Tetsuya Takimoto, Katsuya Suzuki, Tetsuya Miwa, and Yasushi Noguchi*

Frontier Research Laboratories, Institute for Innovation, Ajinomoto Co. Inc., 1-1 Suzuki-cho, Kawasaki-ku, Kawasaki-shi, 210-8681, Japan

Supporting Information

ABSTRACT: Petasin (**1**), a natural product found in plants of the genus *Petasites*, has beneficial medicinal effects, such as antimigraine and antiallergy activities. However, whether or not **1** modulates metabolic diseases is unknown. In this study, the effects of **1** on AMP-activated protein kinase (AMPK), which is considered a pharmacological target for treating metabolic diseases, are described. It was found that an extract of *Petasites japonicus* produces an increase in the phosphorylation of AMPK in vitro, and the main active compound **1** was isolated. When this compound was administered orally to mice, activation of AMPK in the liver, skeletal muscle, and adipose tissue was observed. Moreover, pretreatment with **1** enhanced glucose tolerance following the administration of a glucose solution to normal mice. The mechanism by which **1** activates AMPK was subsequently investigated, and an increased intracellular AMP/ATP ratio in the cultured cells treated with **1** occurred. In addition, treatment with petasin inhibited mitochondrial respiratory chain complex I. Taken together, the present results indicated that **1** modulates glucose metabolism and activates AMPK through the inhibition of mitochondrial respiration. The preclinical data suggested that petasin (**1**) could be useful for the treatment of metabolic diseases in humans.

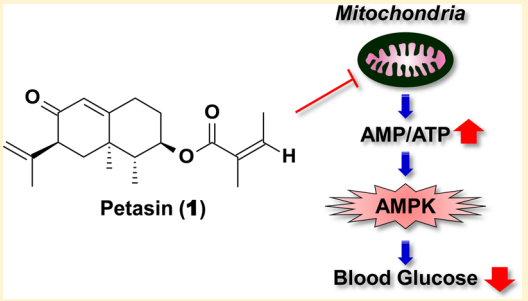

AMP-activated protein kinase (AMPK) is a pharmacological target for the treatment of metabolic diseases such as type 2 diabetes, hyperlipidemia, hypercholesterolemia, and cardiovascular diseases.[1−3] AMPK is a heterotrimeric protein that plays a key role in the regulation of whole-body energy homeostasis and is expressed ubiquitously and senses energy status indicators, such as intracellular adenosine nucleotide ratios, in both individual cells and the entire body.[3] Once activated, AMPK switches on catabolic pathways that generate ATP and switches off pathways that consume ATP. The activation induces an increase in glucose uptake, fatty acid oxidation, and mitochondrial biogenesis and a decrease in lipid synthesis. Thus, AMPK activators may prevent obesity and its related metabolic abnormalities.[3−8] Some insulin-sensitizing drugs, such as biguanides and thiazolidinediones, exert antidiabetic effects through the partial activation of AMPK. Thus, many pharmaceutical companies and research institutions are seeking novel AMPK modulators.[2,9]

Natural products have been a rich source of novel therapeutics for many diseases.[10,11] For decades, the development of AMPK activators from natural products has been reported. Berberine, which is used clinically for the treatment of gut infections and diarrhea, was found recently to have potential for the treatment of diabetes through the activation of AMPK in both human and rodent models.[7] Resveratrol is a stilbene that is isolated from grapes and has potential for the treatment and prevention of cancer, type 2 diabetes, and inflammatory and cardiovascular diseases.[12] Although the underlying mechanism for the beneficial effects of resveratrol is not fully understood, AMPK is thought to be the primary target of resveratrol. In addition, flavonoids and catechins, which show multiple beneficial effects, have been reported to activate AMPK.[13−17]

Therefore, in the present investigation, an attempt was made to isolate new AMPK activators from several plants, and it was found that Fuki shoots (*Petasites japonicus* F. Schmidt) (Asteraceae), which traditionally have been eaten as a vegetable in Japan, displayed potent AMPK activation in cultured cells. Petasin (**1**) is contained not only in *P. japonicus* but also in other *Petasites* species.[18−20] In Europe, *Petasites hybridus* (butterbur) is used therapeutically as an antimigraine, an antiallergy, and a spasmolytic agent for the treatment of inflammatory diseases of the gastrointestinal tract.[20] Consistent with these reports, the beneficial effects of this plant could be the result of the presence of **1** and its derivatives. In the present study, it is shown for the first time that the natural product **1** is a potent AMPK activator in both in vitro and in vivo experiments. Moreover, the mechanism by which **1** activates AMPK has been examined.

Received: October 14, 2013
Published: May 28, 2014

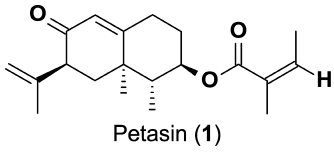

Petasin (**1**)

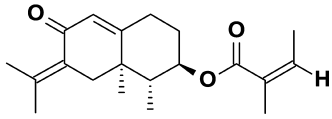

Isopetasin (**2**)

RESULTS AND DISCUSSION

Activation of AMPK by Petasin (1) in H4IIE, 3T3-L1, and C2C12 Cells. It was found that a methanol extract from *P. japonicus* elicited an increase in phosphorylated AMPK in cultured cells. Subsequently, petasin (**1**) and isopetasin (**2**) were shown to be AMPK activators from *P. japonicus* using bioactivity-guided fractionation (Figure 1) and were identified using mass spectrometric and NMR spectroscopic analysis (Figure S1, Supporting Information).

The effects of **1** were focused on because it elicited a greater phosphorylation of AMPK than did isopetasin (**2**) in an in-cell ELISA assay using H4IIE cells (Figure 1A). Next, Western blot analysis was performed to determine whether **1** activates AMPK. As shown in Figure 1B, AICAR (2 mM) (a positive control) increased the phosphorylation of AMPK (Thr172) and ACC (Ser79), of which the latter is downstream of AMPK in the signaling cascade, indicating that AICAR activated AMPKα in the cultured cell lines tested (H4IIE, C2C12, and 3T3-L1 cells). Petasin as well as AICAR demonstrated a dose-dependent increase in phosphorylated AMPKα and ACC in H4IIE cells. The increase was observed in the H4IIE cells treated with **1** for 2 h at a concentration of at least 0.3 μM. It was also confirmed that **1** activated AMPK in other cultured cells, such as 3T3-L1 and C2C12, at concentrations of at least 10 and 5 μM, respectively. These results demonstrated that **1** has potent AMPK-activating effects in cultured H4IIE, C2C12, and 3T3-L1 cells.

Activation of AMPK in Vivo by Petasin (1). Next, it was examined as to whether **1** could activate AMPK in vivo. A single oral administration of **1** was given to normal C57BL/6J mice at a dose of 200 mg/kg body weight. The liver, epididymal white adipose tissue, and skeletal muscle (quadriceps) were immediately removed 2 h after the administration of **1**, and the phosphorylation of AMPK was analyzed by a Western blot analysis. A significant increase was observed in phosphorylated AMPK in the liver of mice treated with **1**, similar to that was observed in the in vitro experiments (Figure 2). It was confirmed also that **1** significantly increased the levels of phosphorylated ACC in the liver, indicating AMPK in the liver to be activated by the administration of **1** (Figure 3A). In white adipose tissue, the phosphorylation of both AMPK and ACC was observed to a similar degree to that observed in the liver (Figures 2 and 3A). Moreover, the phosphorylation of AMPK levels in skeletal muscle increased significantly after the administration of **1** (Figure 2). Unfortunately, data were not obtained for ACC because the Western blot analysis was technically unsuccessful. Therefore, it was decided to examine a downstream molecule other than ACC. AMPK activation was shown to enhance the transcription of the proliferator-activated receptor-γ coactivator-1α (PGC-1α), which regulates the genes involved in energy metabolism including mitochondrial bio-

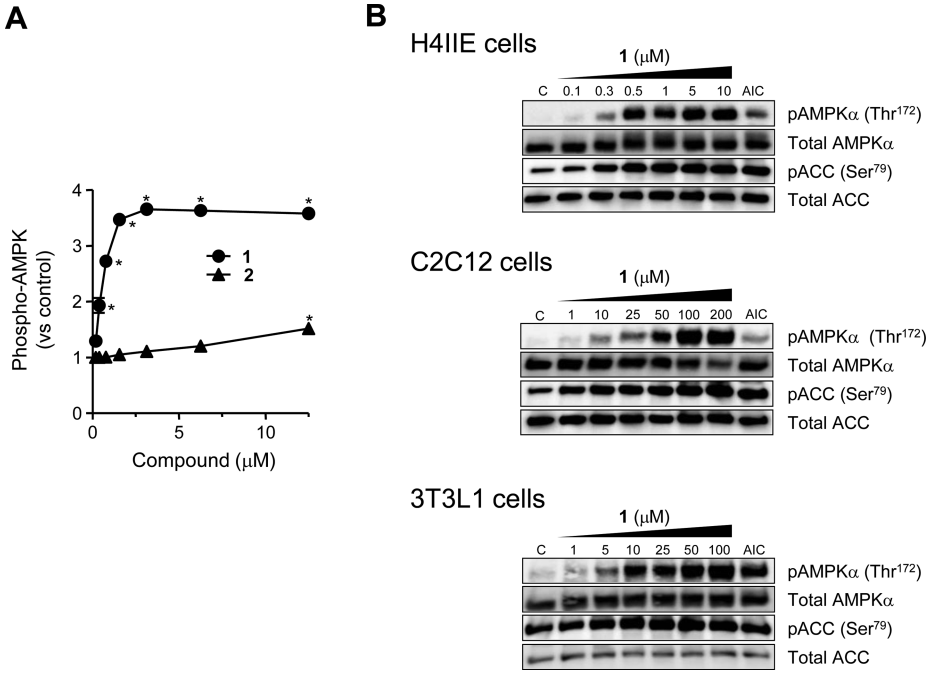

Figure 1. Petasin (**1**), isolated from *P. japonicus*, activates AMPK and ACC in vitro. (A) Following starvation, the H4IIE cells were incubated with the indicated concentrations of **1** or isopetasin (**2**) in 96-well plates at 37 °C for 1 h. The cells were fixed with a 4% formaldehyde solution, and an in-cell ELISA system was utilized to determine the phospho-AMPK (Thr172) levels in the cells [$*p < 0.01$ compared with the basal values (one-way ANOVA and Dunnett's post hoc tests)]. Each symbol is expressed as the mean ± SE ($n = 4$). (B) Following starvation, H4IIE, C2C12, and 3T3-L1 cells were incubated with the indicated concentrations of **1** or 2 mM AICAR (AIC) for 1, 2, and 2 h, respectively. The cell lysates were analyzed via Western blot analysis using anti-phospho-ACC (Ser79) and anti-phospho-AMPK (Thr172) antibodies. The immune-reactive bands were visualized with horseradish peroxidase-conjugated goat anti-rabbit IgG using an ECL detection system.

dx.doi.org/10.1021/np400867m | *J. Nat. Prod.* 2014, 77, 1262−1269

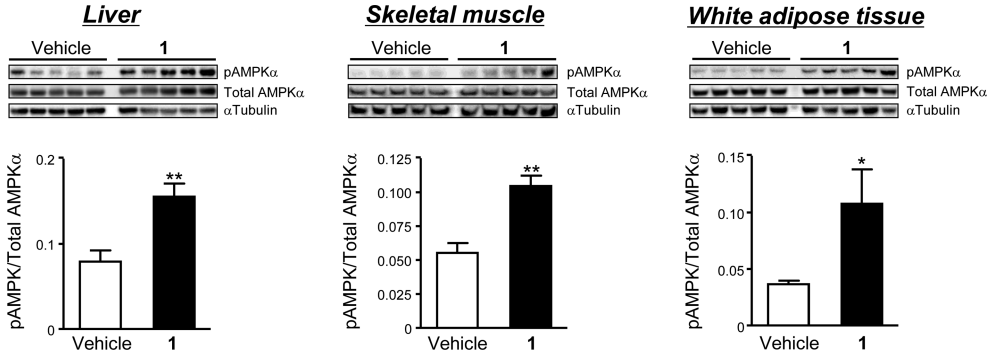

Figure 2. Petasin (**1**) increases the phosphorylation of AMPK in the liver, white adipose tissue, and skeletal muscle of C57BL/6J mice through a single oral administration. Compound **1** (200 mg/kg body weight) was administered orally to C57BL/6J mice that had been fasted for 4 h. After 2 h, the mice were dissected under anesthesia (ip injection of 500 mg/kg body weight chloral hydrate), and the liver, epididymal adipose tissue, and skeletal muscle (quadriceps) were obtained. For the determination of protein expression, Western blot analyses were performed using anti-phospho-AMPKα (Thr172), anti-AMPKα, and anti-α-tubulin antibodies. Each column is expressed as the mean ± SE from 5 mice [$*p < 0.05$ and $**p < 0.01$ compared with the vehicle group (Student's t test)].

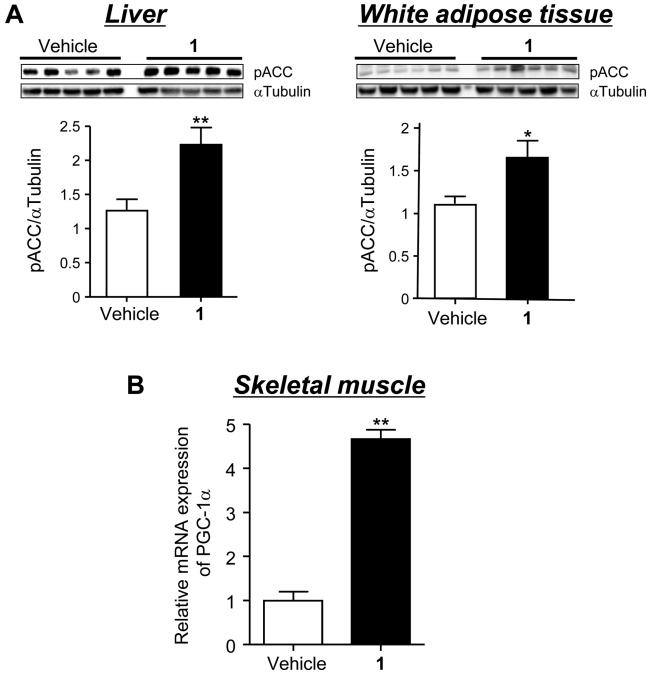

Figure 3. Petasin (**1**) enhances AMPK signaling in the liver, white adipose tissue, and skeletal muscle of C57BL/6J mice through a single oral administration. (A) The expression of the AMPK downstream molecule phospho-ACC (Ser79) in the liver and white adipose tissue was determined using Western blot analyses. The data are normalized to a housekeeping protein (α-tubulin). Each column is expressed as the mean ± SE from 5 mice [$*p < 0.05$ and $**p < 0.01$ compared with the vehicle group (Student's t test)]. (B) Relative mRNA expression of PGC-1α in the skeletal muscle of mice treated with **1**. To determine the mRNA expression of PGC-1α, RT-qPCR was performed. The relative mRNA expression of PGC-1α was normalized to the 18S rRNA.

genesis.[21] Previous reports have shown that AMPK increases the transcription, phosphorylation, and deacetylation of PGC-1α.[22] Although the exact mechanism by which AMPK regulates the expression of PGC-1α has not been established, the interaction between AMPK and multiple steps in the PGC-1α feed-forward regulatory loop has been reported.[22−27] In addition, AMPK activators, such as AICAR or quercetin, have been reported to enhance PGC-1α in skeletal muscle.[28−30] Indeed, in the protocol used, it was confirmed that the transcription of PGC-1α is increased dramatically by a single subcutaneous dose of AICAR (Figure S3, Supporting Information). Therefore, the expression of PGC-1α mRNA rather than ACC was measured to determine whether the **1**-mediated phosphorylation of AMPK affected downstream signals. Two hours after the administration of petasin, PGC-1α mRNA expression was increased in the skeletal muscles as compared with control mice (Figure 3B), suggesting that **1** activates AMPK and affects the downstream signal in the skeletal muscle. These results indicated that **1** activated AMPK in the liver, white adipose tissues, and skeletal muscle. Taken together, it was demonstrated that **1** activated AMPK not only in vitro but also in vivo.

Thus, it was demonstrated for the first time that **1** strongly activates AMPK in the liver, white adipose tissue, and skeletal muscle, which are associated strongly with glucose and lipid metabolism. In general, the activation of AMPK leads to enhanced glucose uptake, fatty acid oxidation, and mitochondrial biogenesis, and it suppresses hepatic glucose production and lipogenesis through the regulation of downstream molecules in the liver and skeletal muscle.[3] However, the roles of AMPK in the white adipose tissue are not fully understood, and according to some reports, the activation of AMPK can increase glucose uptake and fatty acid oxidation, while decreasing lipogenesis and lipolysis in the white adipose tissue, liver, or muscle.[31] Recent studies have suggested that AMPK in white adipose tissue might regulate the secretion of adipocytokines such as TNFα, IL-6, and adiponectin.[32,33] Thus, the effects of AMPK in each of these tissues would ameliorate metabolic diseases through the regulation of glucose and lipid metabolites. Given these facts, the suppressive effect of **1** on blood glucose levels could be caused by the activation of AMPK. Accordingly, an oral glucose tolerance test (OGTT) was performed using C57BL/6J mice to examine the effects of **1** on glucose metabolism. Petasin (**1**) was administered orally in doses of 100 and 200 mg/kg body weight prior to glucose loading. In this experiment, resveratrol, which is known to be an AMPK activator, was used a positive control instead of AICAR because AICAR is not effective orally. During the OGTT, the administration of a glucose solution increased the blood glucose levels in normal mice (Figure 4A). In contrast, the natural AMPK activator resveratrol inhibited the increase in blood glucose levels upon glucose administration in healthy

dx.doi.org/10.1021/np400867m | J. Nat. Prod. 2014, 77, 1262−1269

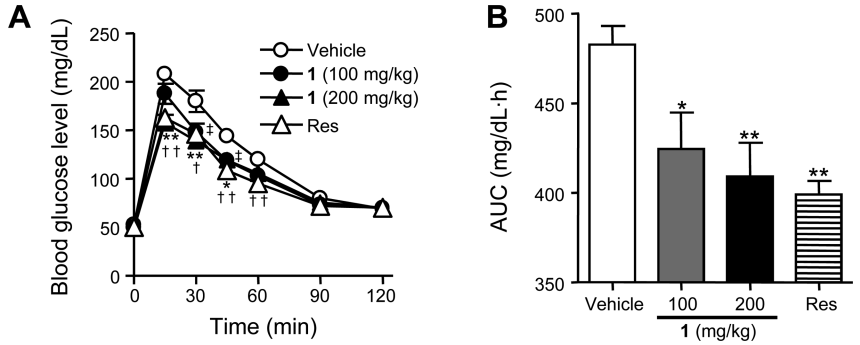

Figure 4. Petasin (**1**) enhances glucose metabolism in C57BL/6J mice through a single oral administration. To examine whether **1** affects glucose metabolism, oral glucose tolerance tests (OGTT) were performed on the mice treated with **1** at doses of 100 mg/kg body weight (-●-) and 200 mg/kg body weight (-▲-) or resveratrol (Res) at a dose of 500 mg/kg body weight (-△-). The vehicle group is indicated using open circles (-○-). The C57BL/6J mice were fasted for 15 h, and **1** was then administered orally at doses of 100 or 200 mg/kg body weight. At 1 h after administration, a glucose solution at a dose of 1 g/kg body weight was administered to the mice. The graph on the left shows the changes in the blood glucose levels in the mice, and the graph on the right indicates the area under the curve (AUC) calculated using the data from the left graph. Data are expressed as the means ± SE from 5 mice [$^{\ddagger}p < 0.05$: 100 mg/kg petasin (**1**) group vs the vehicle group; $^{*}p < 0.05$ and $^{**}p < 0.01$: 200 mg/kg petasin (**1**) group vs the vehicle group; $^{\dagger}p < 0.05$ and $^{\dagger\dagger}p < 0.01$: the resveratrol group vs the vehicle group (one-way ANOVA and Dunnett's post hoc tests)].

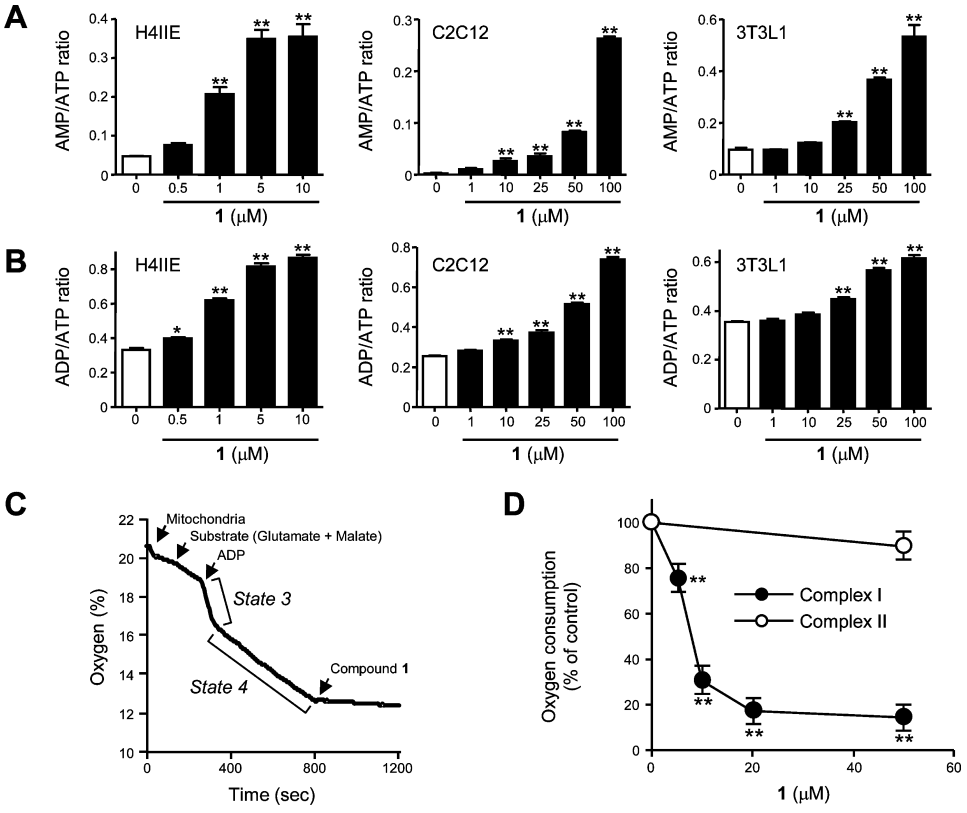

Figure 5. Petasin (**1**) increases the intracellular AMP/ATP and ADP/ATP ratios through inhibiting mitochondrial respiration. (A and B) H4IIE, C2C12, and 3T3-L1 cells were treated with petasin (**1**) for 1, 2, and 2 h, respectively. The AMP/ATP (A) and ADP/ATP (B) ratios were calculated using the data given in Table S1 (Supporting Information). The data are expressed as mean ± SE ($n = 3$) [$^{*}p < 0.05$ and $^{**}p < 0.01$ compared with the untreated cells (one-way ANOVA and Dunnett's post hoc tests)]. (C) Hepatic mitochondria were isolated from normal Wistar rats as described in the Experimental Section. The oxygen concentration in an assay buffer gradually decreased following the addition of the isolated mitochondria and substrates (5 mM glutamate and 2.5 mM malate). When ADP (100 μM) was added to the mitochondria, mitochondrial "State 3" and "State 4" respiration was induced. The administration of **1** (20 μM) suppressed the oxygen decrease in the assay buffer, indicating that **1** inhibited mitochondrial respiration. (D) The dose−response effects on mitochondrial respiration were determined in the presence of 100 μM ADP using substrate combinations targeting either complex I (5 mM glutamate and 2.5 mM malate) or complex II (5 mM succinate and 2 μM rotenone) of the respiratory chain. The data are expressed as means ± SE ($n = 3$) [$^{**}p < 0.01$ compared with the control values (one-way ANOVA and Dunnett's post hoc tests)].

mice. Similarly, a reduction in blood glucose levels was observed after glucose loading in mice treated with **1** at doses of 100 and 200 mg/kg body weight. The AUCs were significantly lower in the mice treated with **1** than in the vehicle group (Figure 4B). These data indicated that **1** acutely enhanced glucose tolerance in normal mice.

dx.doi.org/10.1021/np400867m | J. Nat. Prod. 2014, 77, 1262−1269

Mechanism of AMPK Activation by Petasin (1). To determine the mechanism by which **1** activates AMPK, the concentration of intracellular adenosine nucleotides was examined, such as ATP, ADP, and AMP, in cultured cells. In all of the cultured cells used in the present study, **1** caused a concentration-dependent decrease in the intracellular ATP levels and increased the intracellular AMP and ADP levels (Table S1, Supporting Information). The intracellular AMP/ATP and ADP/ATP ratios were calculated, which are parameters associated with the activation of AMPK. As shown in Figure 5A and B, the AMP/ATP and ADP/ATP ratios increased in a dose-dependent manner in parallel with the activation of AMPK by **1** in H4IIE, C2C12, and 3T3-L1. On the basis of these results, it was hypothesized that **1** influences mitochondrial functions, because these organelles generate most of the intracellular ATP. To investigate whether the changes in the adenosine nucleotides result from the inhibition of mitochondrial respiration, oxygen consumption was examined in the mitochondria isolated from rat livers.

As shown in Figure 5C, mitochondrial oxygen consumption dramatically increased upon the addition of ADP in the presence of glutamate (State 3). Subsequently, mitochondrial respiration advanced to State 4. The administration of 10 μM petasin (**1**) inhibited oxygen consumption at State 4 in the mitochondria in the presence of glutamate, indicating that this compound (**1**) interacted with a mitochondrial component. Since some AMPK activators, such as metformin, rosiglitazone, and berberine, are known to inhibit mitochondrial respiratory complex I,[34,35] it was attempted to determine the effects of **1** on complex I. As expected, **1** produced a dose-dependent inhibition of oxygen consumption in the mitochondria in the presence of a complex I-linked substrate (glutamate plus malate) but not a complex II-linked substrate (succinate plus rotenone) (Figure 5D). These results are consistent with previous reports on complex I inhibitors such as metformin, rosiglitazone, and berberine.[34,35] In general, a decrease in intracellular ATP activates AMPK concomitant with an increase in AMP.[36] Recent studies have proposed that an elevated intracellular AMP level displayed direct allosteric effects and activated AMPK indirectly by preventing the dephosphorylation of Thr172.[3,35] Moreover, ATP was found to antagonize the effects of AMP, suggesting that a change in the AMP/ATP ratio, rather than a change in AMP concentration, controls AMPK activity.[37] Thus, an increase in the AMP/ATP ratio can increase the activation of AMPK and lead to the phosphorylation of downstream substrates. From these results, an increased AMP/ATP ratio was observed in cells treated with **1**, suggesting that this event is the primary mechanism by which **1** activates AMPK.

On the other hand, it has long been known that liver kinase B1 (LKB1) and calmodulin-dependent protein kinase kinase-β (CaMKKβ) can activate AMPK; they are the primary upstream molecules of AMPK. To examine whether **1** might affect LKB1, HeLa cells lacking LKB1 were used (Figure S4, Supporting Information). Since **1** activated AMPK, even in these HeLa cells, this compound does not affect LKB1. However, in a recent paper, it has been reported that an increase in the ADP/ATP ratio in HeLa cells enhanced the ability of agents to increase intracellular calcium levels and to activate AMPK,[37] suggesting that the ADP/ATP ratio is associated with AMPK activation. In the present experiments, it was observed that **1** increased the ADP/ATP ratio in the cultured cells (Figure 5B). Therefore, **1** might activate AMPK through CaMKKβ via changes in the ADP/ATP ratio. Further investigations would be required to determine this exact mechanism.

In conclusion, it was found that petasin (**1**), which was isolated from *P. japonicus* shoots, is a newly determined AMPK activator. An increase of the intracellular AMP/ATP ratio through the inhibition of mitochondrial complex I is the mechanism by which **1** activates AMPK. Moreover, it was observed that **1** prevented an increase in blood glucose levels following loading of a glucose solution and that it activated the downstream targets, such as ACC and PGC-1α, via the activation of AMPK (Figure 6).

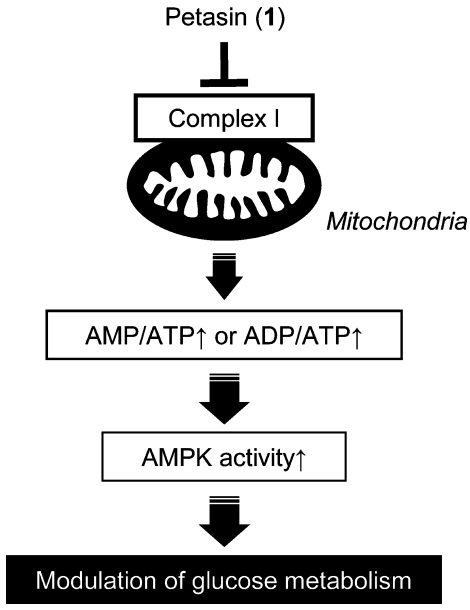

Figure 6. Schematic illustration of the effects of petasin (**1**) on metabolism. Compound **1** suppresses mitochondrial respiration through the inhibition of mitochondrial complex I. The inhibition of mitochondrial respiration decreases the production of ATP, which is followed by an increase in the AMP/ATP and ADP/ATP ratios. Consequently, AMPK is activated through the increase in the AMP/ATP and ADP/ATP ratios in the cells. The activation of AMPK would subsequently affect the metabolism, including that of carbohydrates or lipids, through its interactions with downstream molecules in the signaling pathway.

■ EXPERIMENTAL SECTION

General Experimental Procedures. The ^{1}H and ^{13}C NMR data were acquired on a Bruker Avance 400 NMR spectrometer (Bruker BioSpin Co., Karlsruhe, Germany) using $CDCl_3$ as a solvent. The MS (ion source energy = 40 eV) was recorded on a Quattro micro LC-MS spectrometer (Nihon Waters K.K., Tokyo, Japan). High-resolution mass spectra were obtained using a Q-Tof Premier mass spectrometer (Nihon Waters K.K).

Plant Material. The shoots of *P. japonicus* were obtained from Tsuruoka-shi, Yamagata, Japan, in June 2010 and taxonomically identified by R.S. A voucher specimen (V262) has been deposited in the Institute for Innovation, Ajinomoto Co. Inc., Japan.

Extraction and Isolation. The dried shoots of *P. japonicus* were extracted overnight with methanol at room temperature. After filtration and evaporation of the methanol under reduced pressure, the crude extract was suspended in a small excess of distilled water and partitioned with ethyl acetate to generate dried ethyl acetate-soluble and water-soluble fractions, respectively. The ethyl acetate-soluble fraction was found to activate AMPK in the H4IIE cells, whereas the water-soluble fraction did not. Therefore, the AMPK activators from

the ethyl acetate-soluble fraction were isolated by subjecting two fractions to column chromatography over silica gel, by elution with a stepwise hexane−ethyl acetate solvent system, and subsequently washing it with methanol to obtain nine fractions. Among the resultant fractions, fraction 3 activated AMPK in H4IIE cells. Fraction 3 was further purified using HPLC (Inertsil ODS-3 20 × 250 mm column, flow rate = 10 mL/min, methanol−water, 8:2) to yield three subfractions (3-1, 3-2, and 3-3). Subfraction 3-2 was further purified using HPLC (Inertsil SIL100 20 × 250 mm column, flow rate = 10 mL/min, hexane−ethyl acetate, 9:1) to yield petasin (**1**) (23 mg) and isopetasin (**2**) (7 mg). These compounds exhibited ^{1}H and ^{13}C NMR and ESIMS data consistent with literature values.[19,38,39] The purity of these compounds was determined as >95% as determined by HPLC.

Animals. Male C57BL/6J mice (10 weeks old) and Wistar rats (8 weeks old) were purchased from Charles River Laboratory, Inc., Japan. All animals were maintained in a temperature-controlled room (21 ± 1 °C) on a 12 h light/dark cycle with unlimited access to food and water. All experiments were reviewed and approved by the Animal Care Committee of Ajinomoto Co., Inc. (protocol numbers 2010005 and 2010258) and were performed in accordance with the relevant guidelines.

Cell Culture. Cultured H4IIE hepatoma cells were grown in Dulbecco's modified Eagle's medium (DMEM) containing 1 g/L D-glucose, 10% fetal bovine serum (FBS), and antibiotics (100 UI/L penicillin and 100 μg/mL streptomycin) at 37 °C in a humidified atmosphere of 5% CO_2. The H4IIE cells were cultured in a medium with 10% FBS to ∼80% cell confluence and assayed following overnight serum depletion. The C2C12 fibroblasts were cultured in DMEM containing 4.5 g/L glucose, 10% FBS, and antibiotics. Upon reaching ∼80% confluence, the 10% FBS was replaced with 2% horse serum. Then, 4 days later, assays were performed using well-differentiated myotubes. The 3T3-L1 preadipocytes were cultured in DMEM containing 4.5 g/L glucose and 10% calf serum. At confluence, the cells were differentiated upon incubation in a medium containing 4.5 g/L glucose, 10% FBS, 1.7 μM insulin, 1 μM dexamethasone, and 500 μM isobutyl-1-methylxanthine (IBMX). After 3 days, the medium was changed to DMEM containing 4.5 g/L glucose, 10% FBS, and 1.7 μM insulin. The differentiated adipocytes were used in the experiments 10−14 days after the initiation of differentiation.

In-Cell ELISA Assay for Phospho-AMPK. The H4IIE cells were seeded on 96-well plates and cultured to confluency. Subsequently, the cells were starved overnight in DMEM (1 g/L glucose) without FBS. The medium was then changed to fresh DMEM without FBS, and petasin (**1**) or isopetasin (**2**) was added at the concentrations described in Figure 1B. After the incubation with **1** or **2**, the medium was immediately changed to a 4% formaldehyde solution, and the cells were fixed by incubation at room temperature for 10 min. To deactivate the intrinsic peroxidase, the fixed cells were incubated with a 0.6% H_2O_2 solution for 30 min. After being washed with PBS containing 0.1% Tween 20 (PBS-T), the cells were incubated in 10% FBS at room temperature for 1 h. The cells were then incubated overnight with rabbit anti-p-AMPKα (Thr172) monoclonal antibody (Cell Signaling Technology, Inc., Beverly, MA, USA; 1:400) in a 5% BSA solution at 4 °C. After being washed with 0.1% PBS-T, the cells were incubated with horseradish peroxidase-conjugated goat anti-rabbit IgG (Cell Signaling Technology, Inc.) in a 5% BSA solution at room temperature for 1 h. The immune reactivities were detected using the ELISA POD Substrate TMB kit HYPER (Nacalai Tesque, Inc., Kyoto, Japan).

Western Blot Analysis. The cells treated with **1** or other reagents were lysed in a solution (10 mM Tris-HCl, 4% SDS, and 20% glycerol, pH 6.8) supplemented with protease and phosphatase inhibitors (Nacalai Tesque, Inc.). The liver, quadriceps muscle, and epididymal adipose tissue (approximately 100 mg) from mice treated with **1** were homogenized using a Polytron homogenizer (Capital Scientific, Inc., Austin, TX, USA) in a cold RIPA buffer (25 mM Tris-HCl, 150 mM NaCl, 0.1% SDS, 0.5% sodium deoxycholate, and 1% Nonidet P-40, pH 7.6) supplemented with protease and phosphatase inhibitors. The homogenates were incubated on ice for 10 min and centrifuged at 15000*g* for 10 min to remove tissue debris. The supernatants were stored at −80 °C until further analysis. The protein concentrations were determined using a Bradford assay (Bio-Rad, Hercules, CA, USA). The samples were then heat-denatured in an SDS-PAGE sample buffer at 95 °C for 3 min. Approximately 50−100 μg of protein was loaded and separated using 7.5% SDS-PAGE electrophoresis (gel thickness: 1.5 mm) and electrotransferred (SDS-PAGE) onto a polyvinylidene difluoride membrane. Immunoblotting was performed using the following antibodies purchased from Cell Signaling Technology, Inc.: anti-p-AMPKα (Thr172) (1:1000 dilution), anti-p-ACC (Ser79) (1:1000 dilution), anti-AMPKα (1:1000 dilution), and anti-ACC (1:1000 dilution). The immune-reactive bands were visualized with horseradish peroxidase-conjugated goat anti-rabbit IgG using an ECL detection system (GE Healthcare Japan, Tokyo, Japan). The detection was performed on an LAS-3000 luminescent image analyzer (Fujifilm, Tokyo, Japan).

Determination of Intracellular Adenosine Nucleotide Levels by HPLC. The intracellular adenosine nucleotide concentration was determined as previously reported,[40] with minor modifications made. Thus, after treatment with **1**, the cells were washed with Dulbecco's phosphate-buffered saline once and lysed in a buffer containing 10 mM Tris-HCl (pH 6.8), 4% SDS, and 20% glycerol. To improve sample handling, the RNA was digested with TurboNuclease (Accelagen, Inc., San Diego, CA, USA) at 37 °C for 15 min. Following digestion, 4% perchloric acid was added, and the lysates were incubated on ice for 30 min. The pH of the lysates was adjusted to approximately 7 with 3 M KCO_3. The precipitated salt was separated from the liquid phase using centrifugation at 13000*g* for 10 min at 4 °C. The determination of the adenine nucleotide levels in the lysates was conducted using HPLC (XL-C series; JASCO, Tokyo, Japan) with an ACQUITY-UPLC T3 column (1.8 μm, 2.1 × 150 mm, C_{18} ODS; Nihon Waters, Tokyo, Japan). The nucleotides were detected spectrophotometrically at 290 nm and eluted at a flow rate of 0.2 mL/min at 40 °C. The HPLC buffer contained 20 mM KH_2PO_4 and 3.5 mM K_2HPO_4 at pH 6.2. The presence of ATP, ADP, and AMP was detected at approximately 3, 4, and 7 min, respectively.

Liver Mitochondrial Isolation and Respiration Measurement. The isolation of mitochondria and respiration measurements were performed as previously reported.[41] Each liver was obtained from rats weighing 250 g and quickly placed in an ice-cold mitochondrial isolation medium (10 mM Tris-MOPS, 1 mM EGTA/Tris, and 200 mM sucrose, pH 7.4). The liver (5−8 g) was minced, washed twice with isolation buffer, and carefully homogenized using a glass−Teflon Potter-Elvehjem homogenizer at 1000 rpm. To remove the cell debris, the homogenate was centrifuged at 600*g* for 10 min at 4 °C. Following the addition of isolation buffer, the supernatant was removed and centrifuged at 7000*g* for 10 min at 4 °C. The pellet was washed and recentrifuged at 7000*g* for 10 min at 4 °C, and the resulting pellet was resuspended in an appropriate quantity of isolation buffer. Respiration measurements were conducted on the isolated mitochondria using a Clark-type polarographic oxygen electrode (YSI 5300A Biological Oxygen Monitor; YSI Inc., Yellow Springs, OH, USA). The respiratory control ratios (State 3/State 4 respiration, determined using 5 mM glutamate as a substrate) were 5−7, indicating well-coupled mitochondria. The dose−response effects on the mitochondrial respiration were determined in the presence of 100 μM ADP using substrate combinations targeting either complex I (5 mM glutamate and 2.5 mM malate) or complex II (5 mM succinate and 2 μM rotenone) of the respiratory chain.[7]

In Vivo Measurement of AMPK Activity. The C57BL/6J mice were fasted for 4 h and orally administered petasin (**1**) (200 mg/kg body weight) in 0.5% carboxymethyl cellulose containing 0.5% polyoxyethylene sorbitan. After 2 h, the mice were dissected under anesthesia via ip injection of chloral hydrate (500 mg/kg body weight). The tissues were quickly removed, immediately frozen in liquid nitrogen, and stored at −80 °C until further analysis. For the determination of protein expression, Western blot analyses were performed.

Analysis of mRNA by Quantitative RT-PCR (RT-qPCR). The total RNA was isolated using TRIzol (Invitrogen, Carlsbad, CA, USA). For RT-qPCR analysis, 0.6 μg total RNA was reverse-transcribed with

oligo(dt) using ReverseAid M-MuLV reverse transcriptase. The target cDNA levels were quantified by real-time PCR using the Thermal Cycler Dice Real Time System (Takara Bio Inc., Shiga, Japan). Each reaction tube contained template, 0.5 μM each primer, and SYBR Premix Ex *Taq*II (Takara Bio Inc.). The real-time PCR conditions were as follows: 40 cycles of 95 °C for 5 s and 60 °C for 30 s. The following primer sequences were used to amplify the PGC-1α: 5′ATGTGTCGCCTTCTTGCTCT3′ (sense) and 5′CACGACCTGTGTCGAGAAAA3′ (antisense).

Oral Glucose Tolerance Test. To examine whether petasin (**1**) affects glucose metabolism, an OGTT was performed in mice treated with this compound through a single oral administration. The C57BL/6J mice were fasted for 15 h and orally administered **1** at doses of 100 or 200 mg/kg body weight. After 60 min, a 1 g/kg body weight dose of a 1 M glucose solution was administered to the mice. Blood samples were obtained from the tail vein at 0, 15, 30, 45, 60, 90, and 120 min after glucose administration. The blood glucose levels were measured using a GLUCOCARD meter (Arkray, Kyoto, Japan).

Statistical Analysis. The data are expressed as the means ± SE. The statistical analyses were performed using a one-way analysis of variance (ANOVA) with the Dunnett's multiple comparison post hoc test or Student's *t* tests using GraphPad Prism version 4 software (GraphPad Software, Inc., La Jolla, CA, USA). The statistical significance was set at $p < 0.05$ or $p < 0.01$.

■ ASSOCIATED CONTENT

Ⓢ Supporting Information

Isolation and characterization of AMPK activators from dried shoots of *P. japonicus* (Figure S1). Effects of **1** on the intracellular adenosine nucleotides levels in cultured cells (Table S1), effects of AICAR on phosphorylation of AMPK and ACC in C57BL/6J mice (Figure S2), effects of AICAR on PGC-1α expression in C57BL/6J mice (Figure S3), and effects of **1** on AMPK activation in HeLa cells (Figure S4). These materials are available free of charge via the Internet at http://pubs.acs.org.

■ AUTHOR INFORMATION

Corresponding Author

*Tel: (81)44-2448678. Fax: (81)44-2449617. E-mail: yasushi_noguchi@ajinomoto.com.

Notes

The authors declare no competing financial interest.

■ ACKNOWLEDGMENTS

The authors would like to thank Dr. H. Kisaka and Dr. R. Sugiyama for supplying *P. japonicus*. We are grateful to the staff of our animal research center for animal maintenance. We also thank C. Ijichi and N. Ishida of Ajinomoto Pharmaceuticals for their skillful technical assistance.

■ REFERENCES

(1) Fogarty, S.; Hardie, D. G. *Biochim. Biophys. Acta* **2010**, *1804*, 581−591.
(2) Zhou, G.; Sebhat, I. K.; Zhang, B. B. *Acta Physiol.* **2009**, *196*, 175−190.
(3) Zhang, B. B.; Zhou, G.; Li, C. *Cell Metab.* **2009**, *9*, 407−416.
(4) Buhl, E. S.; Jessen, N.; Pold, R.; Ledet, T.; Flyvbjerg, A.; Pedersen, S. B.; Pedersen, O.; Schmitz, O.; Lund, S. *Diabetes* **2002**, *51*, 2199−2206.
(5) Song, X. M.; Fiedler, M.; Galuska, D.; Ryder, J. W.; Fernstrom, M.; Chibalin, A. V.; Wallberg-Henriksson, H.; Zierath, J. R. *Diabetologia* **2002**, *45*, 56−65.
(6) Cool, B.; Zinker, B.; Chiou, W.; Kifle, L.; Cao, N.; Perham, M.; Dickinson, R.; Adler, A.; Gagne, G.; Iyengar, R.; Zhao, G.; Marsh, K.; Kym, P.; Jung, P.; Camp, H. S.; Frevert, E. *Cell Metab.* **2006**, *3*, 403−416.
(7) Lee, Y. S.; Kim, W. S.; Kim, K. H.; Yoon, M. J.; Cho, H. J.; Shen, Y.; Ye, J. M.; Lee, C. H.; Oh, W. K.; Kim, C. T.; Hohnen-Behrens, C.; Gosby, A.; Kraegen, E. W.; James, D. E.; Kim, J. B. *Diabetes* **2006**, *55*, 2256−2264.
(8) Kitada, M.; Kume, S.; Imaizumi, N.; Koya, D. *Diabetes* **2011**, *60*, 634−643.
(9) Yun, H.; Ha, J. *Expert Opin. Ther. Pat.* **2011**, *21*, 983−1005.
(10) Newman, D. J.; Cragg, G. M. *J. Nat. Prod.* **2007**, *70*, 461−477.
(11) Li, J. W.; Vederas, J. C. *Science* **2009**, *325*, 161−165.
(12) Baur, J. A.; Pearson, K. J.; Price, N. L.; Jamieson, H. A.; Lerin, C.; Kalra, A.; Prabhu, V. V.; Allard, J. S.; Lopez-Lluch, G.; Lewis, K.; Pistell, P. J.; Poosala, S.; Becker, K. G.; Boss, O.; Gwinn, D.; Wang, M.; Ramaswamy, S.; Fishbein, K. W.; Spencer, R. G.; Lakatta, E. G.; Le Couteur, D.; Shaw, R. J.; Navas, P.; Puigserver, P.; Ingram, D. K.; de Cabo, R.; Sinclair, D. A. *Nature* **2006**, *444*, 337−342.
(13) Hwang, J. T.; Park, I. J.; Shin, J. I.; Lee, Y. K.; Lee, S. K.; Baik, H. W.; Ha, J.; Park, O. J. *Biochem. Biophys. Res. Commun.* **2005**, *338*, 694−699.
(14) Collins, Q. F.; Li, H. Y.; Pii, J.; Liu, Z.; Quon, M. J.; Cao, W. *J. Biol. Chem.* **2007**, *282*, 30143−30149.
(15) Cai, E. P.; Lin, J. K. *J. Agric. Food Chem.* **2009**, *57*, 9817−9827.
(16) Zygmunt, K.; Faubert, B.; MacNeil, J.; Tsiani, E. *Biochem. Biophys. Res. Commun.* **2010**, *398*, 178−183.
(17) Ahn, J.; Lee, H.; Kim, S.; Park, J.; Ha, T. *Biochem. Biophys. Res. Commun.* **2008**, *373*, 545−549.
(18) Chizzola, R.; Langer, T.; Franz, C. *Planta Med.* **2006**, *72*, 1254−1256.
(19) Bickel, D.; Roder, T.; Bestmann, H. J.; Brune, K. *Planta Med.* **1994**, *60*, 318−322.
(20) Lipton, R. B.; Gobel, H.; Einhaupl, K. M.; Wilks, K.; Mauskop, A. *Neurology* **2004**, *63*, 2240−2244.
(21) Sandri, M.; Lin, J.; Handschin, C.; Yang, W.; Arany, Z. P.; Lecker, S. H.; Goldberg, A. L.; Spiegelman, B. M. *Proc. Natl. Acad. Sci. U.S.A.* **2006**, *103*, 16260−16265.
(22) Canto, C.; Gerhart-Hines, Z.; Feige, J. N.; Lagouge, M.; Noriega, L.; Milne, J. C.; Elliott, P. J.; Puigserver, P.; Auwerx, J. *Nature* **2009**, *458*, 1056−1060.
(23) McGee, S. L.; Hargreaves, M. *Clin. Sci.* **2010**, *118*, 507−518.
(24) Potthoff, M. J.; Boney-Montoya, J.; Choi, M.; He, T.; Sunny, N. E.; Satapati, S.; Suino-Powell, K.; Xu, H. E.; Gerard, R. D.; Finck, B. N.; Burgess, S. C.; Mangelsdorf, D. J.; Kliewer, S. A. *Cell Metab.* **2011**, *13*, 729−738.
(25) Czubryt, M. P.; McAnally, J.; Fishman, G. I.; Olson, E. N. *Proc. Natl. Acad. Sci. U.S.A.* **2003**, *100*, 1711−1716.
(26) Mair, W.; Morantte, I.; Rodrigues, A. P.; Manning, G.; Montminy, M.; Shaw, R. J.; Dillin, A. *Nature* **2011**, *470*, 404−408.
(27) McGee, S. L.; van Denderen, B. J.; Howlett, K. F.; Mollica, J.; Schertzer, J. D.; Kemp, B. E.; Hargreaves, M. *Diabetes* **2008**, *57*, 860−867.
(28) Lagouge, M.; Argmann, C.; Gerhart-Hines, Z.; Meziane, H.; Lerin, C.; Daussin, F.; Messadeq, N.; Milne, J.; Lambert, P.; Elliott, P.; Geny, B.; Laakso, M.; Puigserver, P.; Auwerx, J. *Cell* **2006**, *127*, 1109−1122.
(29) Leick, L.; Fentz, J.; Bienso, R. S.; Knudsen, J. G.; Jeppesen, J.; Kiens, B.; Wojtaszewski, J. F.; Pilegaard, H. *Am. J. Physiol. Endocrinol. Metab.* **2010**, *299*, E456−E465.
(30) Davis, J. M.; Murphy, E. A.; Carmichael, M. D.; Davis, B. *Am. J. Physiol. Regul. Integr. Comp. Physiol.* **2009**, *296*, R1071−R1077.
(31) Long, Y. C.; Zierath, J. R. *J. Clin. Invest.* **2006**, *116*, 1776−1783.
(32) Lihn, A. S.; Jessen, N.; Pedersen, S. B.; Lund, S.; Richelsen, B. *Biochem. Biophys. Res. Commun.* **2004**, *316*, 853−858.
(33) Ruderman, N. B.; Keller, C.; Richard, A. M.; Saha, A. K.; Luo, Z.; Xiang, X.; Giralt, M.; Ritov, V. B.; Menshikova, E. V.; Kelley, D. E.; Hidalgo, J.; Pedersen, B. K.; Kelly, M. *Diabetes* **2006**, *55* (Suppl. 2), S48−54.

(34) Brunmair, B.; Staniek, K.; Gras, F.; Scharf, N.; Althaym, A.; Clara, R.; Roden, M.; Gnaiger, E.; Nohl, H.; Waldhausl, W.; Furnsinn, C. *Diabetes* **2004**, *53*, 1052−1059.
(35) Turner, N.; Li, J. Y.; Gosby, A.; To, S. W.; Cheng, Z.; Miyoshi, H.; Taketo, M. M.; Cooney, G. J.; Kraegen, E. W.; James, D. E.; Hu, L. H.; Li, J.; Ye, J. M. *Diabetes* **2008**, *57*, 1414−1418.
(36) Carling, D.; Mayer, F. V.; Sanders, M. J.; Gamblin, S. J. *Nat. Chem. Biol.* **2011**, *7*, 512−518.
(37) Hardie, D. G.; Carling, D.; Carlson, M. *Annu. Rev. Biochem.* **1998**, *67*, 821−855.
(38) Matthias, C.; Witschel, H. J. B. *Synthesis* **1997**, *1*, 107−112.
(39) Wildi, E.; Langer, T.; Schaffner, W.; Buter, K. B. *Planta Med.* **1998**, *64*, 264−267.
(40) Fujita, Y.; Hosokawa, M.; Fujimoto, S.; Mukai, E.; Abudukadier, A.; Obara, A.; Ogura, M.; Nakamura, Y.; Toyoda, K.; Nagashima, K.; Seino, Y.; Inagaki, N. *Diabetologia* **2010**, *53*, 1472−1481.
(41) Frezza, C.; Cipolat, S.; Scorrano, L. *Nat. Protoc.* **2007**, *2*, 287−295.